Robotics and Computer-Integrated Manufacturing 25 (2009) 989–998

Contents lists available at ScienceDirect

Robotics and Computer-Integrated Manufacturing

journal homepage: www.elsevier.com/locate/rcim

Chatter detection based on probability distribution of wavelet modulus maxima

Lei Wang [a], Ming Liang [b,*]

[a] Gerdau Ameristeel Corporation, Mississauga, Ontario, Canada
[b] Department of Mechanical Engineering, University of Ottawa, Ottawa, Ontario, Canada

ARTICLE INFO

Keywords:
Chatter detection
End milling
Wavelet transform
Probability distribution
Wavelet modulus maxima
Chatter index

ABSTRACT

This paper presents a statistical chatter detection method. The methodology is based on the study of discrete wavelet transform (DWT) scheme and statistical analysis of wavelet transform modulus maxima (WTMM). Wavelet transform modulus maxima is used to describe any point where wavelet transform of a signal is locally maximal at corresponding time location. Meanwhile, due to the noisy machining environment, a wavelet-based de-noising method including a hybrid thresholding function and a level-dependent universal threshold rule is proposed. A non-dimensional chatter index varying between 0 and 1 is designed based on the statistical analysis of the WTMM. The main advantages of the proposed chatter index include that: (a) its variation range is independent of process parameters and machining systems, and (b) its threshold value is much less susceptible to cutting condition changes since its value is in relative term. As a result, the chatter index could be used for different machining processes without the time-consuming recalibration process.

1. Introduction

Maintaining a reliable and productive machining process is the key to success in metal cutting industry. Chatter, namely the self-excited severe vibration, is considered one of the most important causes of instability in the cutting process. It not only limits productivity of machining processes but also causes poor surface finish, escalated tool wear, and noisy workplace.

Research efforts on delineating the causes of chatter vibration and on its detection have been on-going since as early as 1946. At the early stage, chatter was mostly attributed to negative damping effect [1]. The understanding of chatter mechanism was further enriched by Tobias [2], and Koenigsberger and Tulsty [3] who recognized that the main sources of chatter were the regenerative and mode coupling effects. These effects stem from the interaction of the structural dynamics of the workpiece and machine tool, and the feedback of subsequent cuts of the tool.

Over the past decades, chatter mechanism has been investigated based on Fourier transform (FT) analysis of process signals such as sound pressure [4], force [5], displacement [6], torque [7], or acceleration [8]. These studies have provided valuable insights for future studies. Various chatter indices stemming directly or indirectly from FT spectral analysis have also been proposed for chatter detection. However, since the FT approach conceals all the time-domain information, it is blind to state transition in non-stationary signals and hence ineffective for on-line detection of chatter onset. Though short-time Fourier transform (STFT) could, to certain extent, compensate for this drawback, it is impossible to obtain high resolution in both time and frequency domains [9]. Searching for an acceptable tradeoff between the two for each and every cutting process would be a tedious exercise. This, compounded with its computation-intensive nature, makes it difficult for industrial applications.

To avoid the above difficulties, several on-line calculated chatter indices have been developed. Du et al. [10] applied a ratio between the variances of the filtered force signal and noise in the force signal as a monitoring index. The existence of chatter is signified when the variance ratio is below a certain threshold. Ismail and Kubica [11] proposed an *R*-value, a ratio of root mean squares of the low- and high-frequency components of the cutting force signal for chatter detection. Chatter is detected if the *R*-value reaches a threshold value determined by extensive experimental investigation. Both methods are simple and can reflect the non-stationary nature of cutting force signal. Nevertheless, the use of force signal may undermine their application potential due to the invasive and costly sensors, troublesome setup, and restriction on workpiece size [12]. This has also been acknowledged by Soliman and Ismail [13].

As noted in [10] and further cautioned by Soliman and Ismail [13], it is difficult to specify a proper threshold for many of the chatter indices since they are mostly affected by machining parameters and machining systems. The FT peak amplitude or

* Corresponding author. Tel.: +1 613 562 5800; fax: +1 613 562 5177.
E-mail address: liang@eng.uottawa.ca (M. Liang).

0736-5845/$ - see front matter © 2009 Elsevier Ltd. All rights reserved.
doi:10.1016/j.rcim.2009.04.011

chatter index (CI) values at chatter onset could be quite different in different cutting processes involving different cutters, workpieces and machines. This requires recalibrations of threshold values in response to the changing cutting conditions. Such recalibrations are often time-consuming, knowledge-demanding and are undesirable in a modern manufacturing environment featuring frequent and sometimes unpredictable changes in cutter, machine, and/or work order. This calls for the development of a chatter index that is less susceptible to the variations of cutting processes. For this purpose, Dong et al. [14] and Li et al. [15] applied the coherence function value obtained from two acceleration outputs as a normalized chatter index. The onset of chatter is said to be detected when the coherence value approaches unity. Otherwise, the cutting process is considered to be stable. Since the coherence function value is non-dimensional and is always in the range of (0, 1), theoretically it can be applied to any machining processes. However, to obtain the coherence function value, FT-type computations have to be carried out, which as revealed above may not be suitable for non-stationary signal analysis. Moreover, since the focus of the above reported studies were on turning, the behavior of the coherence-based index in other processes was not examined.

In recent years, some efforts have been made to use wavelet transforms for chatter detection. As compared to other techniques, wavelet transforms possess the advantages in performing local analysis, handling non-stationary or transitory signals, and providing efficient time–frequency analysis. For example, Wu and Du [16] proposed a feature extraction and assessment method by using wavelet packet transform to monitor machining processes. Certain information-rich wavelet packets were used as feature packets. The feature packets were further selected and evaluated. Eventually, the packets with predominant energy are selected for detecting the onset of chatter in turning. When the peak-to-valley values of these predominant packets reach certain threshold, chatter is considered to be detected. Berger et al. [17] employed the ratio of the mean absolute deviations of details d_3 and d_4 of bi-orthogonal wavelets for turning state identification. Choi and Shin [18] proposed a chatter detection methodology using a wavelet-based maximum likelihood (ML) parameter estimation algorithm. A spectral parameter γ was estimated with the maximum likelihood approach and was used as a chatter detection index. The test results of the above approaches are very encouraging and have a great potential for on-line implementation due to their timeliness in chatter onset detection and computational efficiency. Nevertheless, as acknowledged in [18], the threshold values have to be experimentally determined for different cutting processes. The effects of cutter and machine tool on the threshold value remain to be investigated.

The wavelet transform modulus maxima (WTMM) approach has proven to be very effective for the detection of singularities and transient phenomena in image enhancement [19], machine fault monitoring [20], and non-destructive testing [21]. Its ability to detect singularity and pinpoint the temporal location of transients would make it an excellent tool for chatter detection. However, such an application has not yet been reported in the accessible literature. This paper presents a new statistical chatter index based on the distribution of the positive WTMM in an effort to provide an alternative chatter index that is less susceptible to cutting condition changes, and hence should require much less recalibration when used for different processes. In addition, due to the presence of heavy noise in the vibration signal, a hybrid wavelet thresholding method is developed to provide cleaner input for chatter detection.

2. Proposed methodology

2.1. The framework for chatter detection

The proposed methodology is based on discrete wavelet transform (DWT) and statistical analysis of WTMM, i.e., the peak values of wavelet coefficients. The key idea is that the WTMM contain the important information about transient periods and maximum changes such as jumps or singularities in the signal [19]. Therefore, the statistical distribution of these peaks can show different trends or patterns that are used to distinguish faulty condition from normal cutting conditions. Moreover, statistical analysis leads to the formulation of a non-dimensional detection index that overcomes the difficulty present in the empirical specification of the threshold values. The framework of the

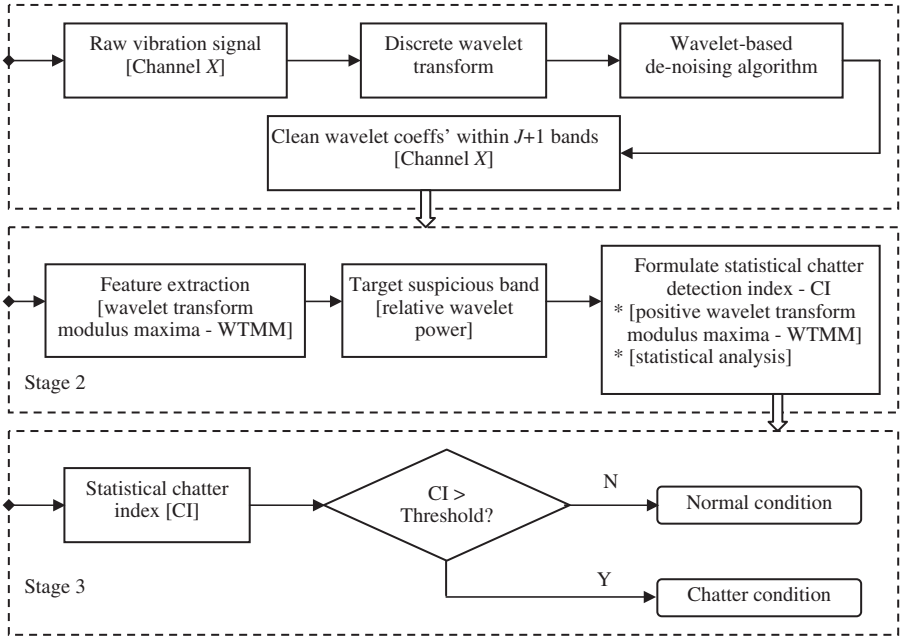

Fig. 1. Flow chart of chatter detection module.

proposed chatter detection scheme is illustrated in Fig. 1. The DWT and wavelet-based de-noising are carried out in stage 1 to decompose the vibration signal into individual frequency bands and to reduce the noise contained in the raw sensing signal. The cleaned wavelet coefficients are then used for feature extraction at stage 2. The chatter features are extracted in terms of WTMM. The suspicious band is targeted according to a relative power discriminating criterion. Consequently, the modulus maxima within the targeted band are used to formulate chatter index via statistical distribution analysis. At stage 3, the final decision on the onset of chatter is made through the comparison of the obtained detection index with a reference value. The theoretical background of the WTMM, the proposed wavelet-based de-noising method, the statistical chatter index, and tests of the proposed method are given in the following sections.

2.2. Wavelet transform and wavelet transform modulus maxima

2.2.1. Wavelet transforms

The continuous wavelet transform (CWT) is defined as follows [9]:

$$W[f(u,s)] = u^{-1/2}\int_{-\infty}^{\infty} f(t)\psi\left(\frac{t-s}{u}\right)dt \tag{1}$$

where $\psi_{u,s}(t) = u^{-1/2}\psi((t-s)/u)$, the functions $\psi_{u,s}(t)$ are called "wavelets" and the function $\psi(t)$ is called "mother wavelet", $f(t)$ is a signal, u and s are scale and location parameters varying continuously over real domain R, respectively.

When we choose $u = u_0^j$, $s = ku_0^j s_0$, where j, k range over integer domain Z, $u_0 > 1$ and $s_0 > 0$ are fixed, then $\psi_{u,s}(t)$ is transformed into

$$\psi_{u,s}(t) = \psi_{j,k}(t) = u_0^{-j/2}\psi\left(\frac{t - ks_0u_0^j}{u_0^j}\right) = u_0^{-j/2}\psi(u_0^{-j}t - ks_0) \tag{2}$$

Consequently, the discrete wavelet transform is obtained [22].

$$W[f(j,k)] = u_0^{-j/2}\int_{-\infty}^{\infty} f(t)\psi(u_0^{-j}t - ks_0)\,dt \tag{3}$$

From the perspective of multi-resolution analysis (MRA) theory to view wavelet transform, a function or signal can be considered as composed of a smooth background and fluctuations or details on top of it. The distinction between the smooth part and the details is determined by the resolution, i.e., by the scale below which the details of a signal cannot be discerned. At a given resolution, a signal is approximated by ignoring all fluctuations below that scale. When the resolution increases progressively, at each stage finer details are added to the coarser description, providing a successively better approximation to the signal. Eventually as the resolution goes to infinity, the exact signal is recovered. Any signal $f(t)$ can be reconstructed by the equation below in any level of scale [23].

$$f(t) = \sum_{j_0=-\infty}^{\infty}\sum_{k=-\infty}^{\infty} c_{j_0,k}\phi_{j_0,k}(t) + \sum_{j=-\infty}^{j_0}\sum_{k=-\infty}^{\infty} d_{j,k}\psi_{j,k}(t) \tag{4}$$

where $c_{j0,k}$ stands for the approximation coefficients at scale j_0 and $d_{j,k}$ represents the detail coefficients at scale j_0 and below. The first part of the above equation is scaling-function dependent approximation of $f(t)$ at scale j_0. The second part of equation contains wavelet-function dependent details of $f(t)$ at scales j_0 and below. The function $\phi_{j,k}(t)$ is called scaling function (or dilation function) in multi-resolution analysis with $\phi_{j,k}(t) = u_0^{-j/2}\phi(u_0^{-j}t - ks_0)$.

As shown in [23], for any given scaling function, the approximation coefficients can be obtained as

$$c_{j,k} = \int_{-\infty}^{\infty} f(t)\phi_{j,k}(t)\,dt \tag{5}$$

Similarly, the detail coefficients can be obtained as

$$d_{j,k} = \int_{-\infty}^{\infty} f(t)\psi_{j,k}(t)\,dt \tag{6}$$

In this study, discrete wavelet transform is adopted because it allows fast signal decomposition, and guarantees both energy conservation and exact signal reconstruction [21]. In particular, the commonly used Daubechies wavelet D_4 [22] is chosen for data transform.

2.2.2. Wavelet transform modulus maxima

As defined in [9], the term "modulus maxima" is used to describe any point (u_0, s_0) such that wavelet transform $|W[f(u, s)]|$ has the locally maximal value at $s = s_0$, here u and s are still the wavelet transform scale and location parameters, respectively, f is a function or signal. At the modulus maxima, the first partial derivatives with respect to s are zero. That is, the modulus maxima are associated with zero-crossing points. Singularities and irregular structures in the signal often carry the most important information such as the information given by transient phenomena like peaks [19]. On the other hand, wavelet transform [9] can focus on localized signal structures and thus the singularities of a signal can be detected.

3. Wavelet-based de-noising algorithm

The vibration signal from the milling machine is usually noisy even during stable cutting. Therefore, an essential step is the purification of the acquired signal. In this study, this is done by thresholding the wavelet coefficients of the signal based on a hybrid thresholding function with a level-dependent threshold rule as detailed in the following.

3.1. The rationale of noise reduction by thresholding wavelet coefficients

Most noise reduction algorithm starts with the following additive model [24]:

$$x(n) = f(n) + \eta(n) \tag{7}$$

where time n is equally spaced, $f(n)$ is a discrete signal of N data and the actual signal $x(n)$ is the same data corrupted with noise $\eta(n)$. $\eta(n)$ is assumed to be independent and identically distributed (IID) Gaussian noise with zero mean ($E\eta = 0$) and standard deviation σ. The de-noising objective is to suppress the noise part of the signal $x(n)$ and to recover $f(n)$. The use of wavelet-based de-noising approach is mainly due to the following considerations:

(1) Small wavelet coefficients are governed by noise, while coefficients with large absolute amplitude values contain more signal information than noise. Hence replacing the smallest, noisy coefficients with zero, the reconstructed signal should retain essential signal characteristics with less noise.
(2) Wavelet decomposition is a multi-scale data representation of original signal. This feature provides a solution in terms of scale-dependent thresholds to correlated noise and is more adaptive to signals that contain different characteristics at different scales.

3.2. An adaptive hybrid thresholding rule

De-noising is commonly done using the hard- or soft-thresholding rule. The hard-thresholding function retains all wavelet coefficient values that are greater than the given threshold and

sets the rest to zero as defined in [25]

$$w_{thr\_h} = \begin{cases} w & |w| \geqslant thr \\ 0 & \text{otherwise} \end{cases} \tag{8}$$

where w denotes noisy wavelet coefficients and thr is the threshold.

The soft-thresholding shrinks the wavelet coefficients by thr if they are greater than thr and the others to zero [25]

$$w_{thr\_s} = \begin{cases} w - thr & w \geqslant thr \\ 0 & |w| < thr \\ w + thr & w \leqslant -thr \end{cases} \tag{9}$$

However, hard-thresholding takes an assertively keep-or-remove approach that may falsely classify a true signal as noise or noise as signal for the inputs around the threshold. On the other hand, the soft-thresholding rule keeps only the portion that is above the threshold and hence may cause serious distortion of the heavily contaminated signal with low signal-to-noise ratio (SNR). The reconstructed signal based on such heavily truncated or shrunk values for signals with low SNR will not represent the true nature of the signal and may leave the chatter undetected due to the large reduction of signal strength.

To alleviate the difficulties present in the above two thresholding rules, an adaptive hybrid thresholding approach is proposed as follows:

$$w_{thr} = \begin{cases} w - \mathrm{sgn}(w)(1-\zeta) \times thr, & |w| \geqslant thr \\ 0, & |w| < thr \end{cases} \tag{10}$$

where ζ is a parameter in the range of (0, 1) and is on-line updated. This thresholding rule is a compromise of the hard and soft approaches since it can be viewed as the linear combination of hard- and soft-thresholding functions in the form of $\zeta \cdot w_{thr\_h} + (1-\zeta) \cdot w_{thr\_s}$. On the other hand, it is adaptive since the weights of hard and soft, represented by ζ and $(1-\zeta)$, are on-line adjusted to reflect the dynamics of the cutting conditions.

The universal threshold [26] is adopted in the adaptive hybrid thresholding rule, i.e.,

$$thr = \sigma\sqrt{2\log(N)} \tag{11}$$

where N is the length of signal, σ is standard deviation of noise at each scale and can be estimated on each scale separately by the median of absolute deviation (MAD) value [27]

$$\hat{\sigma} = \frac{\mathrm{MAD}}{0.6745} \tag{12}$$

To determine ζ, the commonly used mean square error (MSE) could be used as the criterion. The MSE in terms of threshold value is defined in the wavelet domain as follows [24]:

$$MSE(thr) = \frac{1}{N}\|\eta_{thr}\|^2 \tag{13}$$

where $\eta_{thr} = w_{thr} - w_0$, w_0 is noise-free wavelet coefficients and w_{thr} is the wavelet coefficients after thresholding. However, it is impossible to know the "pure" signal $f(n)$ and hence w_0 beforehand. As a result, the MSE function can never be computed exactly. For this reason, the generalized cross validation (GCV) function is used to approximate MSE [24] as follows:

$$MSE \approx GCV(thr) = \frac{1/N \cdot \|w - w_{thr}\|^2}{(N_0(thr)/N)^2} \tag{14}$$

where w is the noisy wavelet coefficient, w_{thr} is the threshold wavelet coefficient, and $N_0(thr)$ stands for the number of noisy wavelet coefficients below the threshold. For each data input cycle, ζ^*, i.e., the optimum ζ that minimizes GCV is used in the adaptive hybrid rule. ζ^* is obtained numerically based on Eq. (14) for each scale.

3.3. Procedure of wavelet-based de-noising algorithm

The proposed de-noising method consists of the following three steps:

Step 1: Signal decomposition

Choose a wavelet function and decompose the underlying signal x. Wavelet coefficients including approximation and detail ones at each level are obtained consequently.

Step 2: Thresholding detail coefficients

Apply the adaptive hybrid thresholding rule to the detail coefficients at each scale level.

Step 3: Reconstruction

Perform inverse wavelet transform using the resultant approximation coefficients and the de-noised detail coefficients for every scale.

4. Chatter feature extraction and index formulation

After de-noising, feature extraction by signal processing methods is the most important step to assess the process state. The extracted features from measured signals should potentially show the highest possible correlation to the states of the monitored phenomenon.

The magnitude of the de-noised wavelet coefficients within each frequency band reflects the amplitude of vibration signal over a time interval. Also as stated earlier, the WTMM carry the vital information of the signal characteristics. Large magnitude components, i.e., modulus maxima, will be present at the time when maximum changes in the signal have occurred. At the chatter onset, the energy of the signal converges to one or a few frequency bands [15] that account for large portion of total energy. In the meantime, most of the energy accumulated in the band(s) is confined to local maximal wavelet coefficients whose magnitudes become larger as well, while other coefficients are either reduced or diminished to zero. Note that wavelet transform does conserve the total energy that a signal holds [28]. Therefore, it is logical to investigate the WTMM and consider it as a key feature of machining conditions.

To relieve the burden in calibrating the chatter index threshold, the chatter index should be normalized in nature, i.e., it should be non-dimensional and varies between 0 and 1. In addition, the derived index should be sensitive to chatters but less susceptible to other disturbances.

In this study, the chatter index is developed based on the statistical distribution analysis of WTMM. This is due to the following considerations. The measured vibration signals are non-deterministic and unpredictable. Their randomness is best characterized with statistical terms. Besides, statistical analysis can produce a non-dimensional index between 0 and 1 in terms of the cumulative distribution function. Moreover, as mentioned earlier, the WTMM method is able to detect the transient period and hence the onset of chatters.

4.1. Statistical distribution analysis of WTMM

The probability distribution of wavelet coefficients has been approximated using a generalized Gaussian distribution [29], Gaussian [30], or Gaussian processes with zero mean [31]. In particular, as studied in [18] wavelet coefficients were modeled as mutually independent Gaussian zero-mean random variables. Consequently, a chatter index was obtained based on a wavelet-based maximum likelihood estimation algorithm. It should be pointed out that the Gaussian processes with non-zero mean can be easily converted into zero-mean Gaussian processes. Therefore,

the wavelet coefficients in this research are also modeled as random variables following Gaussian distribution. $w_{thr}(t)$ is used to denote the Gaussian random process, random variable w_{thr} represents the wavelet coefficients obtained after thresholding and a_p denotes the WTMM with *positive* magnitude. In the next two sub-sections, we will first demonstrate that the WTMM with positive amplitude, i.e., the positive peak values of wavelet coefficients, that exceed level a follow Rayleigh distribution. Then we extend the Rayleigh distribution to Weibull distribution to handle more general cases.

4.2. Rayleigh distribution of WTMM

To show that the positive peak values of the wavelet coefficients follow Rayleigh distribution, the crossing analysis is carried out. It begins with counting the number of "cycles" of wavelet coefficients $w_{thr}(t)$ that have amplitudes greater than $w_{thr}=a$ during period T as illustrated in Fig. 2. From the figure, it can be observed that there are totally six crossings with positive slope that exceed the level $w_{thr}=a$ in time T. Now consider Fig. 2 as one sample function of an ensemble of functions that constitute the stationary random process $w_{thr}(t)$. Let $n_a^+(T)$ denote the number of positive slope crossings of $w_{thr}=a$ in period T and $N_a^+(T)$ be the mean value of $n_a^+(T)$ of all samples, then

$$N_a^+(T)=E[n_a^+(T)] \tag{15}$$

Since the process is stationary, the same result can be obtained if a second interval of duration T is taken immediately after the first. Considering these two intervals together, the following relation holds:

$$N_a^+(2T)=2N_a^+(T) \tag{16}$$

The above equation indicates that for a stationary process the average number of crossings is proportional to T, i.e.,

$$N_a^+(T)=\nu_a^+T \tag{17}$$

where ν_a^+ is the average frequency of crossings at $w_{thr}=a$ with positive slope. ν_a^+ can be derived from the probability distribution of w_{thr} and the result is in terms of the joint probability density function $p(w_{thr}, w'_{thr})$ of random variables w_{thr} and its derivative w'_{thr}

$$\nu_a^+=\left[\int_0^\infty p(w_{thr},w'_{thr})w'_{thr}\,dw'_{thr}\right]_{w_{thr}=a}=\int_0^\infty p(a,w'_{thr})w'_{thr}\,dw'_{thr} \tag{18}$$

Eq. (18) is applicable to any probability distribution of $w_{thr}(t)$. As indicated earlier, the bivariate random variables (w_{thr}, w'_{thr}) approximately follow joint Gaussian distribution. Thus from Eq. (18) we obtain

$$\nu_a^+=\frac{1}{2\pi\sigma_{w_{thr}}\sigma_{w'_{thr}}}e^{-a^2/2\sigma^2_{w_{thr}}}\int_0^\infty e^{-w'^2_{thr}/2\sigma^2_{w'_{thr}}}w'_{thr}\,dw'_{thr} \tag{19}$$

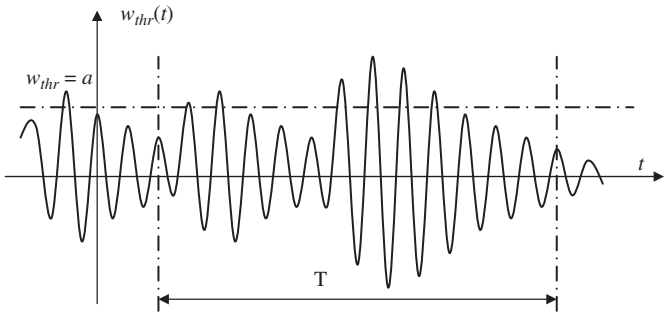

Fig. 2. Sample of a stationary random process of wavelet coefficients.

where $\sigma_{w_{thr}}$ and $\sigma_{w'_{thr}}$ are the standard deviations of random variables w_{thr} and w'_{thr}, respectively. Because

$$\int_0^\infty [e^{-w'^2_{thr}/2\sigma^2_{w'_{thr}}}]w'_{thr}\,dw'_{thr}=\frac{1}{2(1/2\sigma^2_{w'_{thr}})}\times\int_0^\infty e^{-w'^2_{thr}/2\sigma^2_{w'_{thr}}}d\left(\frac{w'^2_{thr}}{2\sigma^2_{w'_{thr}}}\right)=\sigma^2_{w'_{thr}} \tag{20}$$

Eq. (19) becomes

$$\nu_a^+=\frac{\sigma_{w'_{thr}}}{2\pi\sigma_{w_{thr}}}e^{-a2/2\sigma^2_{w_{thr}}} \tag{21}$$

A special case occurs if the level a is equal to zero. It gives a statistical average frequency for crossing level $w_{thr}=0$ (zero-crossing) and is denoted as ν_0^+

$$\nu_0^+=\sigma_{w'_{thr}}/2\pi\sigma_{w_{thr}} \tag{22}$$

Having obtained the frequency of crossings of $w_{thr}=a$, the probability distribution of positive peak wavelet coefficients can be determined by extending the above calculation. Positive peak wavelet coefficients are corresponding to WTMM. Let a_p be the magnitude of a positive peak and $p(a_p)da_p$ be the probability of a peak with positive magnitude randomly chosen in the range a to $a+da_p$. Then the probability that any peak is above a is

$$\text{Prob}(a_p\geqslant a)=\int_a^\infty p(a_p)\,da_p \tag{23}$$

Now during time period T, there will be only an average of ν_a^+T out of ν_0^+T cycles (since one positive crossing of $w_{thr}=0$ occurs for each full cycle of the process) that will have peak values exceeding a. Then, the proportion of cycles whose peak value exceeds a is ν_a^+/ν_0^+ and this is equivalent to the probability that a positive peak value is above a, i.e.,

$$\text{Prob}(a_p\geqslant a)=\int_a^\infty p(a_p)\,da_p=\nu_a^+/\nu_0^+ \tag{24}$$

Differentiating Eq. (24) with respect to a gives

$$-p(a_p)=\frac{1}{\nu_0^+}\frac{d}{da}(\nu_a^+) \tag{25}$$

Eq. (25) is a general result and applicable to any probability density distribution for the occurrence of positive peaks. However, if the random process is Gaussian, there is a simple and important result for $p(a_p)$. Substituting Eq. (21) with $a=a_p$ and (22) into Eq. (25) gives

$$p(a_p)=\frac{a_p}{\sigma^2_{w_{thr}}}e^{-a_p^2/2\sigma^2_{w_{thr}}}\quad 0\leqslant a_p\leqslant\infty \tag{26}$$

Obviously Eq. (26) shows the probability density function of Rayleigh distribution. Since the cumulative distribution function of Rayleigh distribution is $\text{Prob}(a_p<a)=P(a)=1-e^{-a^2/2\sigma^2_{w_{thr}}}$, the probability of any positive peaks a_p exceeding a is

$$\text{Prob}(a_p\geqslant a)=1-P(a)=e^{-a^2/2\sigma^2_{w_{thr}}} \tag{27}$$

The above analysis is associated with those positive peak values of wavelet coefficients. For those peak values of wavelet coefficients with negative magnitudes, if we flip them 180° over the horizontal axis, i.e., taking their absolute values, and do the same crossing analysis, similar results can be obtained in terms of Rayleigh distribution. Mathematically both positive and negative portions of peaks of wavelet coefficients should have same probability distribution. Therefore, only the wavelet transform modulus maxima with positive magnitudes, i.e., those peaks of wavelet coefficients with positive magnitudes, are considered.

4.3. Weibull distribution of WTMM

In the previous section, we have shown that the probability of positive peaks exceeding level a follows Rayleigh distribution. We can also demonstrate that the distribution of the ratio a/a_0 (a_0 is the mean peak height of the positive WTMM) can be described by Weibull distribution. This observation would extend the proposed method to more general applications. Substituting a with a_0, the mean peak height, in Eq. (27) yields

$$\text{Prob}(a_p \geqslant a_0) = e^{-a_0^2/2\sigma_{w_{thr}}^2} = \frac{1}{2} \tag{28}$$

From the above equation, one obtains

$$a_0 = \sigma_{w_{thr}}\sqrt{2\ln 2} \text{ or } \sigma_{w_{thr}} = a_0/\sqrt{2\ln 2} \tag{29}$$

Substituting Eq. (29) into Eq. (27) gives

$$\text{Prob}[(a_p/a_0) \geqslant (a/a_0)] = 1 - P(a/a_0) = e^{-(\ln 2)(a/a_0)^2} \tag{30}$$

Replacing the exponent 2 in Eq. (30) by a general shape parameter γ leads to

$$\text{Prob}[(a_p/a_0) < (a/a_0)] = P(a/a_0) = 1 - e^{-(\ln 2)(a/a_0)^\gamma} \tag{31}$$

The above equation is a cumulative distribution function of Weibull distribution with scale parameter $\alpha = a_0/(\ln 2)^{1/\gamma}$ and zero mean. We then define the $P(a/a_0)$ as chatter index, i.e.,

$$CI = P(a/a_0) = 1 - e^{-(\ln 2)(a/a_0)^\gamma} \tag{32}$$

This is a non-dimensional chatter index in the range of (0,1). It is important to point out that: (a) CI is non-dimensional in the range of (0, 1) and hence it is easier to determine a threshold value; (b) CI is related to WTMM *ratio* rather than the absolute WTMM and so should be less susceptible to changes of processes and machines (When we change processes, the range of WTMM may change substantially but the range of ratio a/a_0 does not change significantly); and (c) CI is based on the WTMM and should be sensitive to chatter (singularities).

4.4. Procedure of chatter detection

It would be more efficient to calculate the $P(a/a_0)$ value for only a target scale or frequency band where the chatter frequency resides. The target scale is identified based on the ratio of power in each band to the total power of all bands. The frequency band with the highest power ratio is considered as the target for scrutiny. Chatter is confirmed only when the chatter index value of the target band exceeds a threshold. The normalized wavelet power (NWP) in band j is calculated as follows [32]:

$$NWP(j) = \frac{1}{M}\sum_{k=0}^{M-1}(w_{thr}^{j,k})^2 \tag{33}$$

where $w_{thr}^{j,k}$ is the de-noised wavelet coefficient in scale j and location k, M is the number of wavelet coefficients in each frequency band, calculated by $M = N/2^j$, N is the total number of data points in each data acquisition cycle. The target scale j^T is

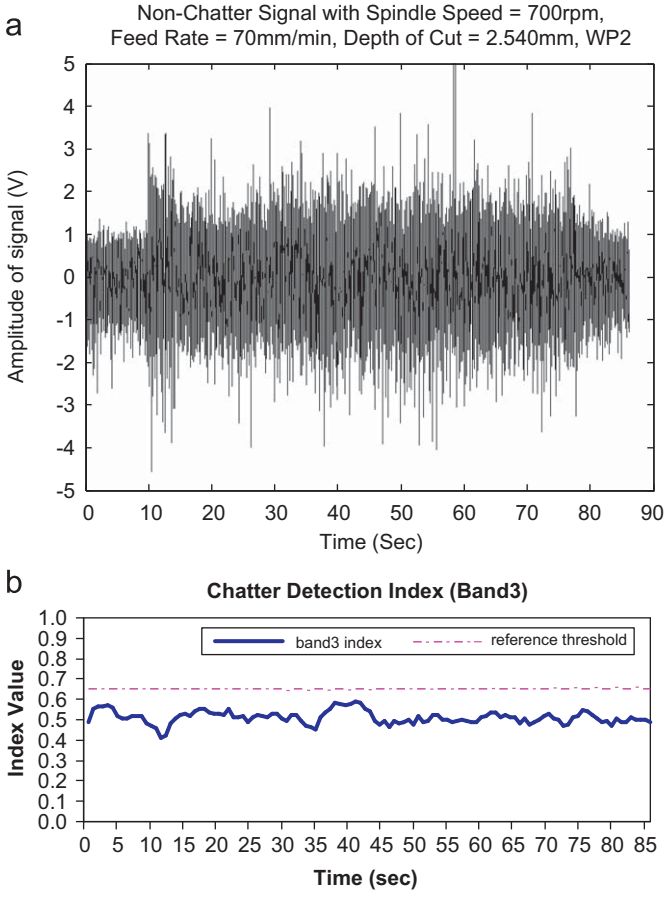

Fig. 4. Chatter detection result of test #1 (Spindle speed 700 rpm, feed rate 70 mm/min, depth of cut 2.54 mm, new cutter): (a) Raw signal; (b) chatter index.

Fig. 3. Experimental setup.

given by

$$j^T = \arg\max_j RP(j) = \arg\max_j \left(NWP(j) / \sum_{j=1}^{J} NWP(j) \right) \quad (34)$$

where J is the total number of scale levels. Then the following procedure is applied to the target scale to identify chatter:

Step 1. Extract WTMM from de-noised wavelet coefficients.

Step 2. Estimate Weibull shape parameter γ and median peak height a_0.

Step 3. Compute CI using Eq. (32).

As the number of samples generally has an influence on the accuracy of parameter estimation, a moving window with a specified size is proposed. Accordingly, with the increased sample size, the index shows clear trend and tends to be smoother.

5. Experimental work

5.1. Experimental setup

The proposed chatter detection methodology has been tested on a CNC SERVO 2000 milling machine (Fig. 3), supplied by Servo Products Co. The spindle of the milling machine is driven by a 3-HP AC motor with a three-phase G3 drive by Saftronics Inc. The x- and y-axis table motions are NC controlled. A Wilcoxon 993B-6 piezoelectric accelerometer is mounted near the tool holder to collect vibration signal. The vibration signal passes through an amplifier and is then sampled and digitized by an NI DAQ AT-MIO-16DE-10 data acquisition card with up to 100 kS/s reading capacity and 12-bit resolution. An Intel Pentium desktop PC is used for signal processing and chatter detection. LabWindows™/CVI is adopted as the development platform for the chatter detection algorithm. The chatter detection system is programmed in C language for on-line implementation. The National Instruments Signal Processing Toolset is used to perform discrete wavelet transform. The LabWindows™ panel is designed to display the collected signal and to conduct chatter detection analysis.

High-Speed Steel (HSS) 3/8 in. (9.525 mm) end-milling cutters with four helical flutes of 30° angle are used for slot cutting of 1018 cold rolled steel workpiece of 20 mm thick, 101 mm long and 76 mm wide (this is the cutting length). Coolant is applied and the tool overhang is set at 38 mm for all tests. The vibration signals are acquired at a sampling rate of 2.0 kHz with a window size of $N = 1024$ samples. The chatter index is computed for every 512 samples. Theoretically, the sequence length determines the number of scale levels in discrete wavelet transform. Here, the data sequence length of $N = 512 = 2^9$ indicates that there should be nine wavelet levels. However, the major concern of this study is to detect chatter occurrence rather than the exact chatter frequency. It is, therefore, not important to decompose the data up to the theoretical scale levels. The number of decomposition levels is therefore set to 5 in this study to reduce computing time and enhance responsiveness to chatter onset.

The tests are conducted using different combinations of spindle speed, feed rate, and depth of cut. The cutting conditions are selected with reference to the recommended parameters for similar cutters [33] to generate stable and unstable cutting conditions. Extensive tests indicate a chatter index threshold, 0.65, can be used to distinguish stable and unstable processes for different machining conditions.

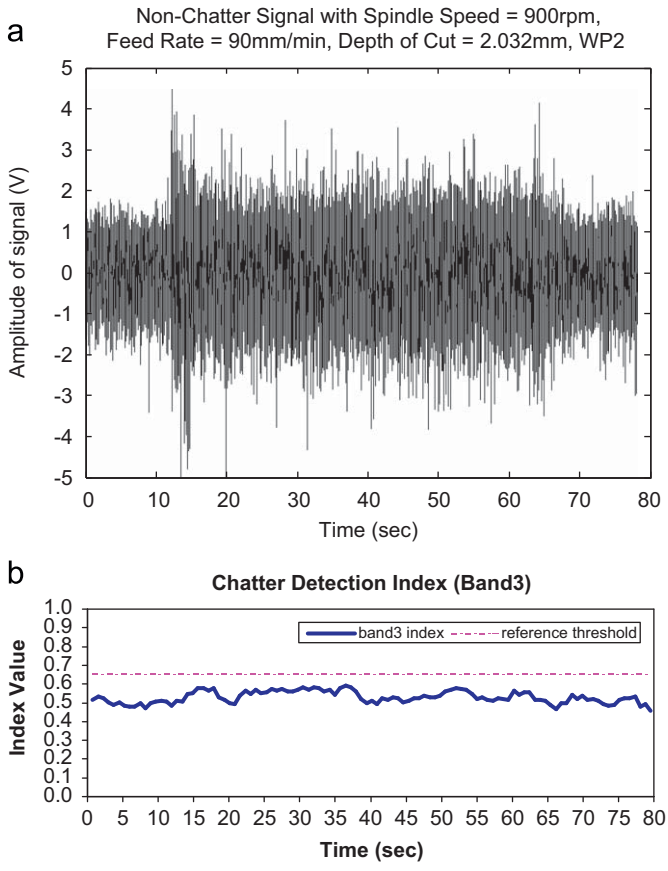

Fig. 5. Chatter detection result of test #2 (Spindle speed 900 rpm, feed rate 90 mm/min, depth of cut 2.032 mm, new cutter): (a) Raw signal; (b) chatter index.

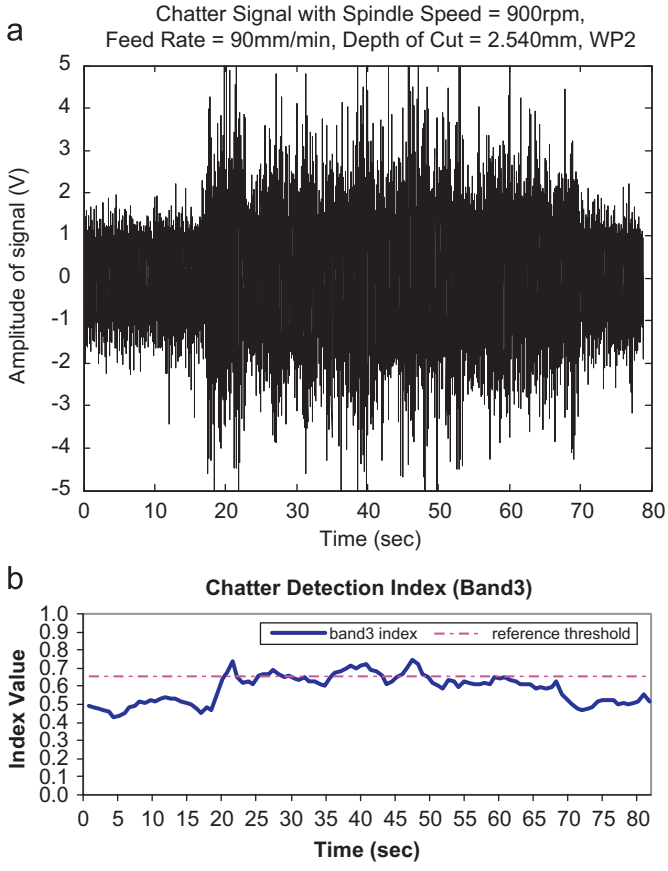

Fig. 6. Chatter detection result of test #3 (Spindle speed 900 rpm, feed rate 90 mm/min, depth of cut 2.54 mm, new cutter): (a) Raw signal, (b) Chatter index.

5.2. Experimental results

Figs. 4–10 display the results for three conditions: stable (Figs. 4 and 5), moderate chatter (Figs. 6 and 7), and severe chatter (Figs. 8–10). It is observed that the CI levels during the stable machining processes are evenly distributed in all frequency ranges or bands and there is no clear dominant frequency band. This is an indication of a stable cutting process [15]. Only one band is presented for each of tests #1 and #2 as shown in Figs. 4 and 5. The on-line calculated CI values are below the threshold value, 0.65.

In tests #3 and #4 (Figs. 6 and 7), moderate chatter is signaled by a CI level that is in the close vicinity of the threshold: 0.60–0.75. Severe chatter vibrations are observed in tests #5, #6, and #7 as shown in Figs. 8–10. The range of the CI values in the critical bands for all the three tests are virtually the same, varying between 0.80 and 0.90, which are significantly higher than the threshold value, 0.65. Such a high CI level clearly indicates the presence of severe chatter. A closer examination of the time-domain signals and CI plots in the critical bands (Figs. 8(b), 9(b) and 10(b)) shows that the chatter onsets (at 21, 15, and 16 s into the cutting processes for tests #5, #6, and #7, respectively) were captured almost immediately for all the three cases.

The above test results suggest that chatter severity could be estimated by the CI value. For example, the CI above 0.75 indicates severe chatter, the CI in the range of 0.6–0.75 reflects moderate chatter, and generally a stable state can be concluded if CI is below 0.60.

5.3. Discussion

5.3.1. System behavior under different cutting conditions

In this study, our tests indicate that chatter is directly related to the depth of cut. For example, the feed rate and spindle speed are identical, i.e., 90 mm/min and 900 rpm, in tests # 2, 3, and 6 but the chatter severities are quite different as, respectively, shown in Figs. 5, 6, and 9 due to the different depths of cut (2.032, 2.540, and 3.048 mm, respectively, for the three tests). The same can be observed by comparing tests #1 (Fig. 4) and #5 (Fig. 8). The feed rate and spindle speed are the same (70 mm/min and 700 rpm, respectively) for both cases, but the depth of cut is increased from 2.540 (test #1) to 3.048 mm (test # 5). Thus the system condition shifts from normal to severe chatter.

Furthermore, the above tests indicate that, even for identical depth of cut, the cutting processes could be either stable or unstable depending on spindle speed and feed rate. Test #1 (Fig. 4) tells us that there is no chatter when depth of cut is 2.540 mm and the speed and feed rate are 700 rpm and 70 mm/min, respectively. However, for the same depth of cut, test #3 (Fig. 6) immediately shows the occurrence of chatter at the spindle speed of 900 rpm and feed rate of 90 mm/min.

5.3.2. Threshold value robustness

As pointed out earlier, the CI value is a probability measure of the occurrence that the WTMM are above a certain level. Its variation range is always between 0 and 1 regardless of the

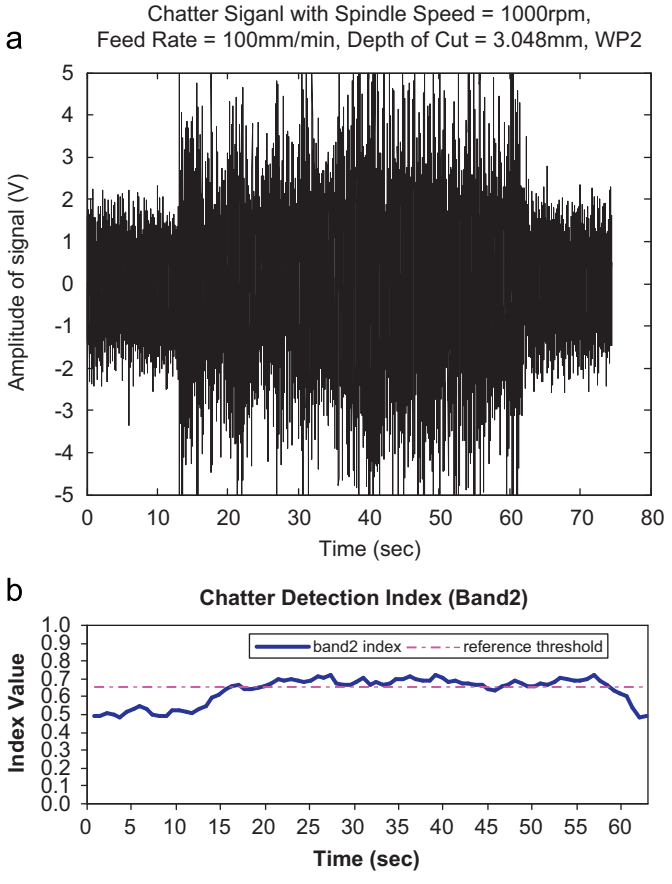

Fig. 7. Chatter detection result of test #4 (Spindle speed 1000 rpm, feed rate 100 mm/min, depth of cut 3.048 mm, partially worn cutter): (a) Raw signal; (b) chatter index.

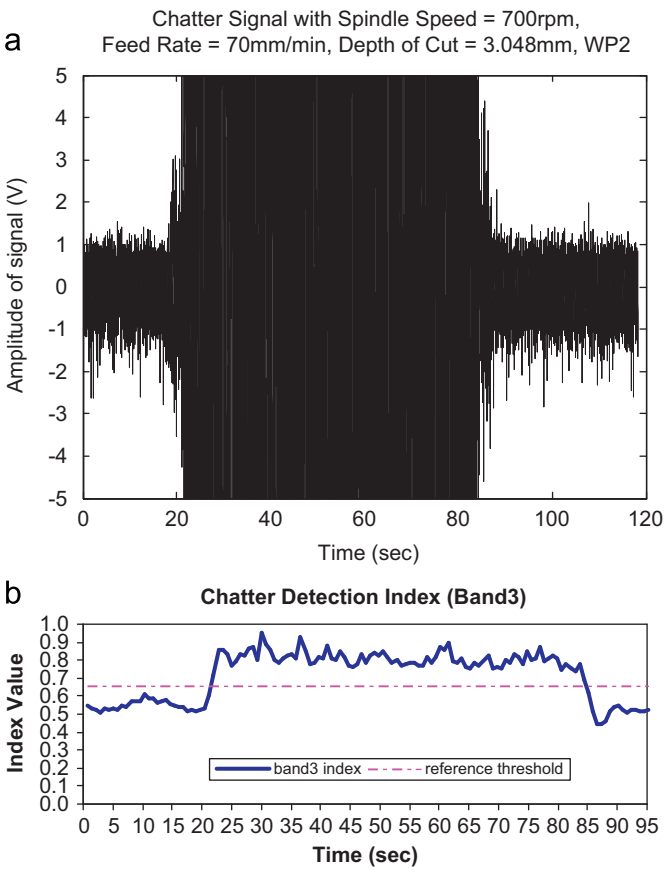

Fig. 8. Chatter detection result of test #5 (Spindle speed 700 rpm, feed rate 70 mm/min, depth of cut 3.048 mm, new cutter): (a) Raw signal, (b) Chatter index.

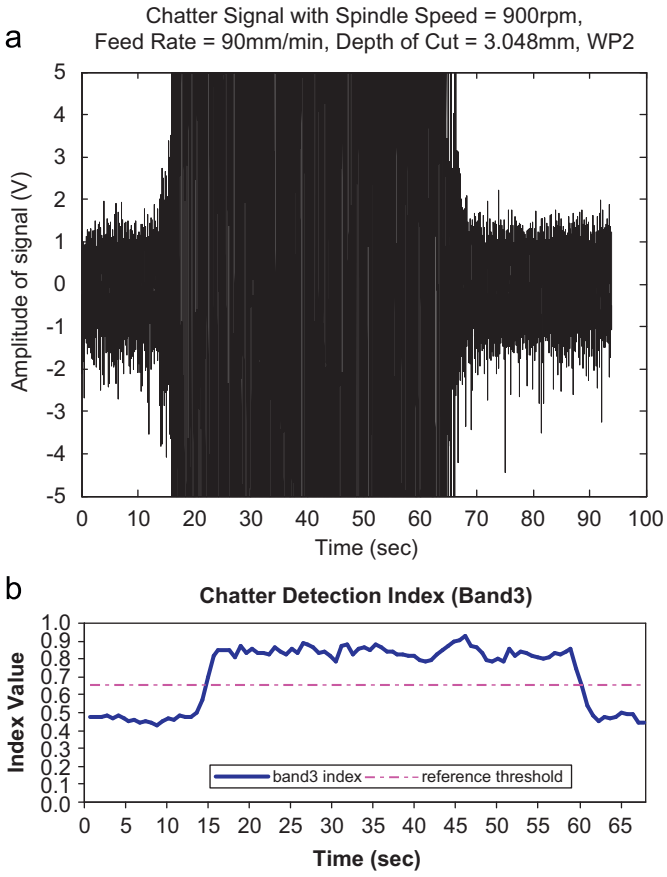

Fig. 9. Chatter detection result of test #6 (Spindle speed 900 rpm, feed rate 90 mm/min, depth of cut 3.048 mm, new cutter): (a) Raw signal; (b) chatter index.

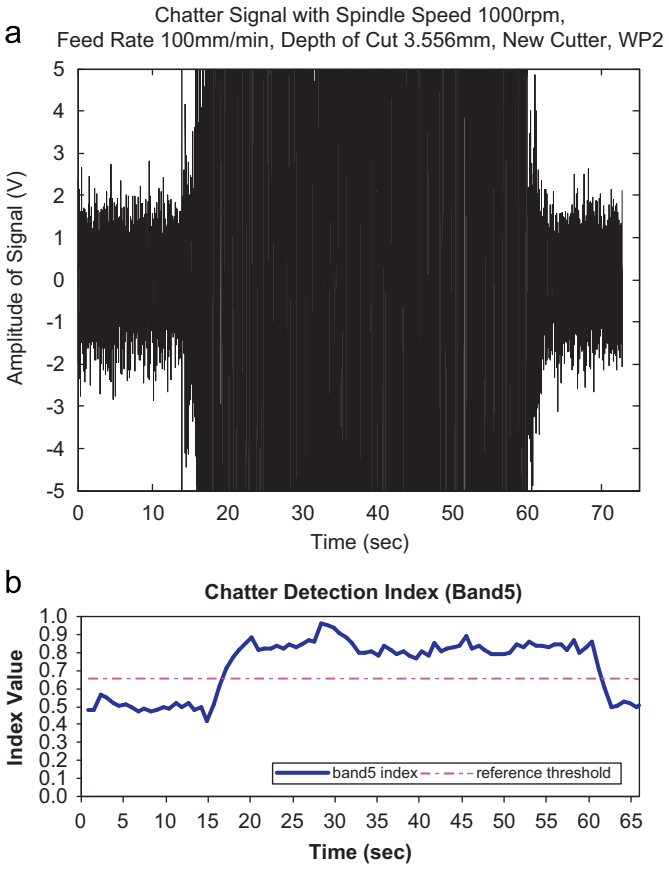

Fig. 10. Chatter detection result of test #7 (Spindle speed 1000 rpm, feed rate 100 mm/min, depth of cut 3.556 mm, new cutter): (a) Raw signal, (b) Chatter index.

changes in machining parameter, tool, workpiece, and machine. Consequently, the threshold is a relative term and should not be susceptible to machining parameter changes either. This was also observed in our tests. The tests were carried out using different spindle speeds varying from 700 to 1000 rpm, feed rates in the range of 70–100 mm/min, and depths of cut from 2.540 to 3.556 mm, and both new and partially worn cutters. As shown above, the same threshold value, 0.65, was used and worked well for all the tests. The insensitivity of the CI threshold to process changes shows a promising potential for general chatter detection applications.

6. Conclusions

A non-dimensional chatter index has been developed based on the wavelet transform modulus maxima (WTMM) and statistical analysis. The advantages of this chatter index includes: (a) it reflects the random and statistical nature of the metal cutting process, (b) it is sensitive to chatters as it is based on WTMM, which is well known to be effective in detecting singularities, (c) it should be less susceptible to process changes because the WTMM ratio instead of the absolute WTMM is used in devising the chatter index, and (d) it varies between 0 and 1 independent of cutting processes and hence can be used in different machining processes. The effectiveness of the proposed method has been tested experimentally.

Acknowledgment

This study was supported by the Natural Science and Engineering Research Council of Canada. This support is greatly appreciated.

References

[1] Arnold RN. The mechanism of tool vibration in the cutting of steel. Proceedings of the Institution of Mechanical Engineers 1946;154:261–84.
[2] Tobias SA, Fishwick W. A theory of regenerative chatter. London: The Engineer; 1958.
[3] Koenigsberger F, Tlusty J. Machine tools structures-—Vol. I: stability against chatter. London: Pergamon Press; 1967.
[4] Altintas Y, Chan PK. In-process detection and suppression of chatter in milling. International Journal of Machine Tools and Manufacturing 1992;32:329–47.
[5] Sastry S, Kapoor SG, DeVor RE. Floquet theory based approach for stability analysis of the variable speed face-milling process. Journal of Manufacturing Science and Engineering 2002;124:10–7.
[6] Bayly PV, Metzler SA, Schaut AJ, Young KA. Theory of torsional chatter in twist drills: model, stability analysis and composition to test. Journal of Manufacturing Science and Engineering 2001;552-561.
[7] Tarng YS, Li TC. Detection and suppression of drilling chatter. ASME Journal of Dynamic Systems, Measurement, and Control 1994;116:729–34.
[8] Wang JH, Lee KN. Suppression of chatter vibration of a CNC machine centre—an example. Mechanical Systems and Signal Processing 1996;10:551–60.
[9] Mallat SG. A wavelet tour of signal processing. London: Academic Press Limited; 1998.
[10] Du RX, Elbestawi M, Li S. Tool condition monitoring in turning using fuzzy set theory. International Journal of Machine Tools and Manufacturing 1992;32:781–96.

[11] Ismail F, Kubica EG. Active suppression of chatter in peripheral milling, Part 1: a statistical indicator to evaluate the spindle speed modulation method. International Journal of Advanced Manufacturing Technology 1995;10: 299–310.
[12] Kim TY, Kim J. Adaptive cutting force control for a machining center by using indirect cutting force measurements. International Journal of Machine Tools and Manufacture 1996;36:925–37.
[13] Soliman E, Ismail F. A control system for chatter avoidance by ramping the spindle speed. Journal of Manufacturing Science and Engineering 1998;120: 674–83.
[14] Dong W, Au Y, Mardapittas A. Machine tool chatter monitoring by coherence analysis. International Journal of Production Research 1992;30:1901–24.
[15] Li XQ, Wong YS, Nee AYC. Tool wear and chatter detection using the coherence function of two crossed accelerations. International Journal of Machine Tools and Manufacturing 1997;37:425–35.
[16] Wu Y, Du R. Feature extraction and assessment using wavelet packets for monitoring of machining processes. Journal of Mechanical Systems and Signal Processing 1996;10:29–53.
[17] Berger BS, Minis I, Harley J, Rokni M, Papadopoulos M. Wavelet-based cutting state identification. Journal of Sound and Vibration 1998;213:813–27.
[18] Choi T, Shin YC. On-line chatter detection using wavelet-based parameter estimation. ASME Journal of Manufacturing Science and Engineering 2003;125:21–8.
[19] Mallat S, Hwang WL. Singularity detection and processing with wavelets. IEEE Transactions on Information Theory 1992;38:617–43.
[20] Miao Q, Makis V. Condition monitoring and classification of rotating machinery using wavelets and hidden Markov models. Mechanical Systems and Signal Processing 2007;21:840–55.
[21] Watson JN, Addison PS. Spectral-temporal filtering of NDT data using wavelet transform modulus maxima. Mechanics Research Communications 2002;29: 99–106.
[22] Daubechies I. Ten lectures on wavelets. Philadelphia: Society for Industrial and Applied Mathematics; 1992.
[23] Erlebacher G, Hussaini MY, Jameson ML. Wavelet: theory and applications. Oxford: Oxford University Press; 1996.
[24] Jansen M. Noise reduction by wavelet thresholding. New York: Springer; 2001.
[25] Debnath L. Wavelets and signal processing. Boston: Birkhauser; 2003.
[26] Donoho DL. De-noising by soft-thresholding. IEEE Transactions on Information Theory 1995;41:613–27.
[27] Vidakovic B. Statistical modeling by wavelets. New York: Wiley; 1999.
[28] Walker JS. A primer on wavelets and their scientific applications. New York: Chapman & Hall/CRC; 1999.
[29] Mallat SG. A theory for multiresolution signal decomposition: the wavelet representation. IEEE Transactions on Pattern Analysis and Machine Intelligence 1989;2:674–93.
[30] Browne M, Cutmore TRH. Low-probability event-detection and separation via statistical wavelet thresholding: an application to psychophysiological denoising. Clinical Neurophysiology 2002;113:1403–11.
[31] Gupta S, Chauhan RC, Sexana SC. Wavelet-based statistical approach for speckle reduction in medical ultrasound images. Medical & Biological Engineering & Computing 2004;42:189–92.
[32] Torrence C, Compo GP. A practical guide to wavelet analysis. Bulletin of the American Meteorological Society 1998;79:61–79.
[33] Meng S. Handbook of metal cutting processes. Beijing: Machinery Industry Press; 1996.